

1 Study of the combined effect of temperature, pH and water activity on
2 the radial growth rate of the white-rot basidiomycete *Physisporinus*
3 *vitreus* by using a hyphal growth model

4

5 M. J. Fuhr^{a,b}, C. Stührk^{a,b}, M. Schubert^a, F. W. M. R. Schwarze^b and H. J. Herrmann^a

6 ^a*ETH Zurich, Institute for Building Materials, Computational Physics for Engineering*
7 *Materials, Schafmattstrasse 6, HIF E18, CH-8093 Zurich, Switzerland*

8 ^b*EMPA, Swiss Federal Laboratories for Materials Science and Technology, Wood*
9 *Laboratory, Group of Wood Protection and Biotechnology, Lerchenfeldstrasse 5, CH-9014 St*
10 *Gallen, Switzerland*

11

12 mfuhr@ethz.ch

13 Chris.Stuehrk@empa.ch

14 Mark.Schubert@empa.ch

15 Francis.Schwarze@empa.ch

16 hans@ifb.baug.ethz.ch

17

18 Corresponding author: M.J. Fuhr. Phone: +41 44 633 7153

19 5 figures, 2 tables

20

21 **Summary**

22 The present work investigates environmental effects on the growth of fungal colonies of *P.*

23 *vitreus* by using a lattice-free discrete modelling approach called FGM (Fuhr & Schubert,

24 2010, arXiv:1101.1747), in which hyphae *and* nutrients are considered as discrete structures.

25 A discrete modelling approach allows studying the underlying mechanistic rule concerning
26 the basic architecture and dynamic of fungal networks on the scale of a single colony. By
27 comparing simulations of the FGM to laboratory experiments of growing fungal colonies on
28 malt extract agar we show that combined effect of temperature, pH and water activity on the
29 radial growth rate fungal colony on a macroscopic scale may be explained by a power law for
30 the growth costs of hyphal expansion on a microscopic scale. The information about the
31 response of the fungal mycelium on a microscopic scale to environmental conditions is
32 essential to simulate its behavior in complex structure substrates such as wood, where the
33 impact of the fungus to the wood (i.e. the degradation of bordered pits or the creation of bore
34 holes and cavities) changes the local environmental condition, e.g. the permeability of the
35 substrate and therefore the water activity level in a colonized pore. A combination of
36 diffusion processes of moisture into wood with the FGM may brighten the knowledge about
37 the colonization strategy of *P. vitreus* and helps to optimize its growth behavior for
38 biotechnological application such as bioincising.

39

40 Keywords: filamentous fungus, fungal colony, mycelia modelling, wood decay fungus

41

42 **1 Introduction**

43 Microorganisms such as wood-decay fungi regulate their metabolism as respond to changing
44 environmental conditions. Environmental factors thereby highly influenced the growth
45 behavior and development of fungal mycelium in wood (Rayner and Boddy, 1988). Schubert
46 et al. (2010) showed that the water activity, temperature and pH are the key factors for the
47 growth behavior of the wood-decay fungi *Physisporinus vitreus* and *Neolentinus lepideus*.
48 The knowledge about the influence of these abiotic factors to the microorganisms is of
49 relevance for biotechnological applications of these wood-decay fungi in bioremediation
50 (Majcherczyk and Hüttermann, 1998; Messner et al., 2002) or bioincising (Lehringer et al.,

51 2009; Schubert and Schwarze, 2009) as well as for the morphogenesis of filamentous fungi in
52 general.

53 The biotechnological process of bioincising is a method for enhancing the
54 permeability of refractory wood by using wood-decay fungi such as *P. vitreus* in order to
55 improve the liquid uptake (e.g. wood-modification agents or resins). The degradation of the
56 bordered pits, which are valve-like connections between the wood pores and closed in
57 Norway spruce heartwood, provides *P. vitreus* as a suitable agent for bioincising in its first
58 stage of growth (Schwarze and Landmesser, 2000; Schwarze et al., 2006). In this growth
59 phase the wood colonization process is accompanied only by slight mass losses and without
60 reducing significantly the strength of the wood (Schwarze et al., 2006). The uptake of wood
61 modification agents can be increased by a factor of 5 depending on the incubation conditions
62 as shown by (Schubert and Schwarze, 2009). The clustered growth pattern of the fungus and
63 its simultaneous growth pattern reported by (Lehringer et al., 2010) observe that the
64 degradation of the pit membranes occurred simultaneously with an attack of the cell wall (i.e.
65 bore holes, cavities and notches). The occurrence of such negative side effects may depend on
66 influencing factors such as nutrient supply and moisture content of the substrate (Lehringer et
67 al., 2010). Therefore the knowledge about the response of the fungus to combined
68 environmental factors is of significance for the biotechnological applications since the
69 optimal growth behavior (i.e. uniformity of wood colonization) is important for upscaling the
70 bioincising process. Mathematical models in combination with laboratory experiments can
71 illuminate the growth behavior of the fungus and may provide an optimization of
72 biotechnological processes under defined conditions.

73 In order to model the response of a single fungal colony on combined effects of
74 environmental factors semi-empirical models based on ordinary differential equations are
75 widely used (Davidson, 2007; Skinner et al., 1994). The response surface (RS) methodology
76 was successfully applied to model the growth of ascomycetes (Begoude et al., 2007; Panagou

77 et al., 2003; Schubert et al., 2010; Schubert et al., 2009) as well as basidiomycete (Schubert et
78 al.). Compared to RS radial basis function (RBF) neural network models, which are based on
79 artificial neural networks, show a better performance to predict specific growth rate in relation
80 to environmental factors (Panagou et al., 2007). By using RBF neural network Schubert et al.
81 (2010) found that the growth of the fungi *P. vitreus* mainly depends on the water activity
82 (0.950 – 0.998) and temperature (10-30 °C), while the pH (4-6) affects the growth rate to a
83 lesser extent. Despite their success the class of models mentioned above is not able to explain
84 the underlying mechanistic rules concerning the basic architecture and dynamic of fungal
85 networks on the scale of a single colony. In particular, recent developments of discrete
86 modelling approaches, in which hyphae are considered as discrete structures, successfully
87 simulate fungal growth in heterogeneous (Boswell, 2008; Boswell et al., 2007) or even
88 complex physically and chemically structured wood-like environments (Fuhr et al., 2010).

89 The present work investigates environmental effects on the growth of fungal colonies
90 of *P. vitreus* by using a lattice-free discrete modelling approach, in which hyphae *and*
91 nutrients are considered as discrete structures. Discrete models of fungal growth have been
92 developed by many authors in the past (Bell, 1986; Cohen, 1967; Ermentrout and Edelstein-
93 Keshet, 1993; Hutchinson et al., 1980; Kotov and Reshetnikov, 1990; Regalado et al., 1996).
94 A review of discrete models is given by Boswell & Hopkins (Boswell and Hopkins, 2009).
95 This class of models is not a substitution for classic modelling approaches such as RS or RBF,
96 but rather a complement to investigate further aspects of hyphal growth on the single colony
97 scale.

98

99 **2 Materials and methods**

100 2.1. Hyphal growth model

101 In order to analyze the growth of filamentous fungi in homogeneous environment, e.g. the
102 growth of fungi on malt extract agar (MEA), we use a two-dimensional implementation of the

103 hyphal growth model introduced by Fuhr et al. (2010). This hyphal growth model is a lattice-
104 free discrete modelling approach for simulating fungal growth in physically and chemically
105 complex structured environment.

106 The model considers the mycelium as an assemblage of nodes, edges and tips. The
107 substrate is formed of point-like nutrient sources. The nodes are connected by edges and form
108 the mycelium, whereby the nodes of the mycelium are restricted to the position of the nutrient
109 points as shown in Fig. 1a. The evolution of the mycelium is driven by key processes, such as
110 polarization, uptake- and concentration of nutrients, and transport of nutrients, determining
111 the morphology of the fungal colony (see Fig. 1b). Details about the model description can be
112 found in Fuhr et al. (2010).

113 In order to model fungal growth on a two-dimensional surface, i.e. the expansion of a
114 colony on MEA, the substrate consists of Poisson distributed nutrient points with ν initial
115 amount of nutrients. Therefore the probability P to find k nutrient points at a specific interval
116 is given by

$$P(k) = \frac{\omega^k}{k!} e^{-\omega}, \quad (1)$$

117 where $\omega > 0$ is a scale parameter of the distribution.

118 The simulation starts by placing n_k^0 starting nodes, called pellets, with an initial
119 nutrient concentration n_n^0 on a circle with diameter n_d^0 millimeter in the centre of a two-
120 dimensional surface of size $L \times L$. The initial nodes have tips with an orientation normal to
121 the circle's surface. At every iteration step m of the algorithm the mycelium is extended by
122 one edge of length l_i at node (i) if its nutrient concentration $f_i^{(m)}$ is larger than the growth costs
123 $\Omega_i^{(m)}$. We assume that the growth costs of the fungus, which may be interpreted as the energy
124 consumption of the metabolic activity of the fungus, increase with lower values of the water
125 activity since the water activity is a measure for the available amount of water for an
126 organism in its environment, e.g. the growth of fungus *P. vitreus* is inhibited below $a_w =$

127 0.966 (Schubert et al., 2010). Dependent on the water activity level Schubert (Schubert et al.,
128 2010) observed a maximal growth rate of the fungus at about 25°C. Below or above this
129 optimum growth temperature the fungal colony expands at a lower rate, i.e. the growth costs
130 are higher. The growth costs may be given by

$$\Omega_i^{(m)} = \left(a \cdot \frac{l_i^{(m)}}{\xi} \right)^b \cdot v, \quad (2)$$

131 where a and b are unknown factors depend of the water activity and the temperature
132 respectively. ξ is the growth cut-off length (Fuhr et al., 2010). The scaling behavior of the
133 unknown factors can be estimated by comparing the simulation with laboratory experiments.

134

135 2.2 Experimental design

136 In order to calibrate and verify the hyphal growth model we use light microscopy. The fungus
137 was cultivated on a glass slide covered with MEA. The experiments were performed with a
138 Zeiss 200M (10× 0.5NA Fluar objective) widefield microscopy (WFM) at room temperature
139 and pH = 6. The growing colony was observed over a time span of 2.5 hours by taking single
140 images of size 1024 × 1024 pixels (48 bit RGB color) with a resolution of approximately 0.78
141 μm per pixel. A 3 x 4 grid of single images built a mosaic image with a total size of 2077 ×
142 4095 pixels. The stitching of the single images to a mosaic image was performed with the
143 AxioVision software package. The mosaic images were taken with a camera (AxioCamMR3)
144 at an interval of 15 minutes. We observe a radial growth rate of the fungal colony of about 2
145 mm per day, which corresponds to a water activity level of the environment of approximately
146 0.990 (Schubert et al., 2010).

147

148 2.3 Measures of the fungal colony

149 Filamentous fungi form a fractal, tree-like structure termed mycelium in order to explore their
 150 environment. By considering the mycelium as a network common network measures can be
 151 applied to study fungal colonies (Fricker et al., 2007).

152

153 Radial growth rate

154 The radial expansion of a fungal colony is often used as a measure for the metabolic activity
 155 of the fungus. We define the radius R of a fungal colony starting form a circular inoculum as

$$R_{95} = \min \left\{ r: \frac{\sum_{(i) \forall (d_i^2 < r^2)}^{N_k} l_i}{\sum_{i=1}^{N_k} l_i} \geq 0.95 \right\}, \quad (3)$$

156 where N_k is the number of nodes, l_i is the total length of mycelium associated with node (i)
 157 and d_i is its distance from the centre of gravity of the inoculum. The radial growth rate G_r is
 158 given by $G_r = dR_{95} / dt$.

159

160 Hyphal growth unit

161 The hyphal growth unit (HGU) is the average length of hypha associated with each tip of
 162 mycelium. First postulated by Plomley (1958), the HGU is defined as

$$HGU = \frac{\sum_{i=1}^{N_k} l_i}{N_t}, \quad (3)$$

163 where N_t is the number of active tips of the mycelium. The HGU depends on the
 164 environmental condition and is constant during unrestricted growth of the mycelium
 165 (Plomley, 1958; Trinci, 1974).

166

167 **3 Results and discussion**

168 The combined abiotic factors temperature, pH and water activity significantly influence the
 169 growth behavior and development of the wood-decay fungus *P. vitreus* as shown in Schubert
 170 et al. (2010). In order to investigate and discuss the underlying mechanism determining the

171 growth behavior of the fungus we calibrate the FGM in a first step (Sec. 3.1) by comparing
172 the microscopic growth pattern of the colony *in vitro* and *in silico*. The obtained parameter set
173 can be use to estimate the parameters a and b of Eq. 2 by comparing the simulation with the
174 laboratory experiments of Schubert et al. (2010) in Sec. 3.2. The knowledge about the scaling
175 behavior of these parameters may be useful to simulate the growing fungus in complex
176 structure environments such as wood, where the activity of the fungus (i.e. the degradation of
177 bordered pits or the creation of bore holes and cavities) changes the local environmental
178 conditions, e.g. the water activity level in a pore.

179

180 3.1 Growth pattern

181 Fig. 2a shows the growth front of *P. vitreus* measured with WFM and Fig. 2b the
182 corresponding simulation by using the parameter set given in Tab. 1. The growth fronts of the
183 colonies expand at room temperature with about $G_r = 2$ millimeters per day, which
184 corresponds to a water activity level of $a_w = 0.990$. We measure the hyphal length of the
185 mycelium, the number of active tips and the HGU of the colony front over a time span of 150
186 minutes within the box in Fig. 2. The results are presented in Tab. 2. We consider only the
187 front of the colony because of the identification of the active tips in the core region of the
188 fungal colony is difficult due to many overlapping layers of mycelium.

189 We observe that hyphae on the colony front growth much faster, than hyphae in the
190 older part of the mycelium. The ratio of the velocities between these classes of hyphae is
191 about 5/1. This effect is considered in the FGM by a lack of nutrients in core of the colony.
192 However, the FGM does not consider an inhibitor, which restricts the growth of the hyphae in
193 the core of the colony.

194 The automated identification of the hyphae measured with WFM is difficult and based
195 on present data especially in the core region of the mycelium not possible. A fluorescent fungi

196 can help to improve the contrast of the images and may an automated segmentation is
197 possible.

198

199 3.2 Radial growth rate

200 Fig. 3 shows the radial growth rate measured at different temperatures and evaluated for four
201 sets of water activity levels, i.e. the water activity levels are 0.998 (circle), 0.990 (triangle),
202 0.982 (square), 0.974 (diamond) and 0.970 (star). The solid lines with the empty symbols are
203 the corresponding simulation of the FGM by fitting the model parameters a and b to the water
204 activity a_w and temperature T respectively. We use $a = \{0, 0.2, 1, 1.8, 6.4\}$ for the water
205 activities levels of $a_w = \{1, 0.998, 0.990, 0.982, 0.974\}$ and for the parameter b in the interval
206 $[0, 4]$ the scaling law $b(T) = 9 + 5 \cdot T$. Therefore we can estimate the model parameters a as
207 function of the water activity a_w as shown in Fig. 5 by

$$a(a_w) = 0.1985 \cdot (e^{134.5 \cdot (1-a_w)} - 1). \quad (4)$$

208 The model parameter a increases exponentially with decreasing water activity levels, while
209 the parameter b depends linearly on the temperature.

210 The model shows, that the radial growth rate increases for higher water activity levels
211 and decreases with lower temperature. For $a = 0$ the growth costs of the fungus vanish and we
212 observe the maximal growth rate of 4.5 millimeters per day. Above approximately $a = 6.4$
213 there is no growth observable within one day, since the growth costs even for small hyphal
214 lengths (i.e. $\frac{l_i^{(m)}}{\xi} \sim 0.16$) are higher than the available nutrients at a nutrient point. Between 10
215 and 25°C the model show a good agreement with quantitative (Fig. 3) and qualitative
216 laboratory experiments (Figs. 2 and 4). Above 25°C the radial growth rate of the mycelium
217 decreases and hyphal growth may be affected by heat shock proteins (Sienkiewicz et al.,
218 1997). The effect of such proteins is not incorporated in our model.

219

220 **4 Conclusion**

221 We analyze the combined effect of temperature, pH and water activity on the radial growth
222 rate of *Physisporinus vitreus* in a homogeneous environment by using a two-dimensional
223 hyphal growth model considering hyphae and nutrients as discrete structures. The simulations
224 show a good qualitative and quantitative agreement with experimental results.

225 We found that combined effect of temperature, pH and water activity on the radial
226 growth rate fungal colony may be explained by growth costs for hyphal expansion on a
227 microscopic scale described by the power law of Eq. 2. The presented model is limited to a
228 temperature range between 5 and 25 °C and a water activity between 0.970 and 1. Above
229 25°C the radial growth rate of the mycelium decreases and hyphal growth may be affected by
230 heat shock proteins. The effect of such proteins is not incorporated in our model.

231 Our results are of significance for biotechnological applications of *P. vitreus* in
232 processes such as bioincising (Schubert and Schwarze, 2009) as well as for the study of
233 filamentous fungi in general. For the process of bioincising, which is a biotechnological
234 approach to improve the uptake of wood-modification substances by harnessing the selective
235 degradation pattern of *P. vitreus*, the knowledge about the response of the fungus to combined
236 abiotic factors is important for successfully designing an optimal incubation procedure.
237 Therefore future studies will focus on modelling the growth of *P. vitreus* in heterogeneous
238 and physically structured two-dimensional wood-like environments.

239

240 **6 Acknowledgements**

241 The authors gratefully acknowledge to J. Hehl for helpful discussions and express their
242 gratitude to the Swiss National Science Foundation (SNF) No. 205321-121701 for its
243 financial support. Imaging was performed on instruments of the ETH Light Microscopy
244 Center.

245

246 **References**

- 247 Begoude, B.A.D., R. Lahlali, D. Friel, P.R. Tondje, and M.H. Jijakli, 2007. Response surface
248 methodology study of the combined effects of temperature, pH, and aw on the
249 growth rate of *Trichoderma asperellum*. *Journal of Applied Microbiology* 103:
250 845-854.
- 251 Bell, A.D., 1986. The Simulation of Branching Patters in Modular Organisms.
252 *Philosophical Transactions of the Royal Society of London B* 313: 143-159.
- 253 Boswell, G.P., 2008. Modelling mycelial networks in structured environments.
254 *Mycological Research* 112: 1015-1025.
- 255 Boswell, G.P., and S. Hopkins, 2009. Linking hyphal growth to colony dynamics: Spatially
256 explicit models of mycelia. *Fungal Ecology* 1: 143-154.
- 257 Boswell, G.P., H. Jacobs, K. Ritz, G.M. Gadd, and F.A. Davidson, 2007. The Development of
258 Fungal Networks in Complex Environments. *Bulletin of Mathematical Biology* 69:
259 605-634.
- 260 Cohen, D., 1967. Computer simulation of biological pattern generation processes. *Nature*
261 216: 246-248.
- 262 Davidson, F.A., 2007. Mathematical modelling of mycelia: a question of scale. *Fungal*
263 *Biology Reviews* 21: 30-41.
- 264 Ermentrout, G.B., and L. Edelstein-Keshet, 1993. Cellular automata approaches to
265 biological modeling. *Journal of Theoretical Biology* 160: 97-133.
- 266 Fricker, M., L. Boddy, and D. Debber, 2007. Network organisation of mycelial fungi.
267 *Biology of the fungal cell* 8: 309-330.
- 268 Fuhr, M.J., M. Schubert, F. Schwarze, and H.J. Herrmann, 2010. Modeling hyphal growth
269 of the wood decay fungus *Physisporinus vitreus*. arXiv:0711.2993.
- 270 Hutchinson, S.A., P. Sharma, K.R. Clarke, and I. Macdonald, 1980. Control of Hyphal
271 Orientation in Colonies of *Mucor Hiemalis*. *Transactions of the British*
272 *Mycological Society* 75: 177-191.
- 273 Kotov, V., and S.V. Reshetnikov, 1990. A stochastic model for early mycelial growth.
274 *Mycological Research* 94: 577-586.
- 275 Lehringer, C., M. Arnold, K. Richter, K. Schubert, F. Schwarze, and H. Miltz. 2009.
276 Bioincised Wood as Substrate for Surface Modification European Conference on
277 Wood Modification 2009.
- 278 Lehringer, C., K. Hillebrand, K. Richter, M. Arnold, F. Schwarze, and H. Miltz, 2010.
279 Anatomy of bioincised Norway spruce wood. *International Biodeterioration &*
280 *Biodegradation* 64: 346-355.
- 281 Majcherczyk, A., and A. Hüttermann, 1998. Bioremediation of wood treated with
282 preservatives using white-rot fungi, p. 129-140, in: A. Bruce and J. W. Palfreyman,
283 Eds.), *Forest products biotechnology*, Taylor and Francis.
- 284 Messner, K., K. Fackler, P. Lamaipis, W. Gindl, E. Srebotnik, and T. Watanabe. 2002.
285 *Biotechnological wood modification*, pp. 45-49. Viena University.
- 286 Panagou, E., V. Kodogiannis, and G. Nychas, 2007. Modelling fungal growth using radial
287 basis function neural networks: The case of the ascomycetous fungus *Monascus*
288 *ruber* van Tieghem. *International Journal of Food Microbiology* 117: 276-286.
- 289 Panagou, E.Z., P.N. Skandamis, and G.J.E. Nychas, 2003. Modelling the combined effect of
290 temperature, pH and aw on the growth rate of *Monascus ruber*, a heat-resistant
291 fungus isolated from green table olives. *Journal of Applied Microbiology* 94: 146-
292 156.
- 293 Plomley, N.J.B., 1958. Formation of the colony in the fungus *Chaetomium*. *Australian*
294 *Journal of Biological Sciences* 12: 53-64.

295 Rayner, A.D., and L. Boddy, 1988. Fungal decomposition of wood: Its biology and ecology
 296 Wiley Chichester and New York.

297 Regalado, C.M., J.W. Crawford, K. Ritz, and B.D. Sleema, 1996. The origins of spatial
 298 heterogeneity in vegetative mycelia: a reaction-diffusion model. *Mycological*
 299 *Research* 100: 1473-1480.

300 Schubert, M., and F. Schwarze, 2009. Response Surface Analyse (RSM) der Wirkung
 301 kombinierter Parameter auf das Wachstum von *Physisporinus vitreus*.
 302 *Holztechnologie* 50: 16-20.

303 Schubert, M., S. Mourad, and F. Schwarze, 2010. Radial basis function neural networks
 304 for modeling growth rates of the basidiomycetes *Physisporinus vitreus* and
 305 *Neolentinus lepideus*. *Applied microbiology and biotechnology* 85: 703-712.

306 Schubert, M., V. Dengler, S. Mourad, and F. Schwarze, Determination of optimal growth
 307 parameters for the bioincising fungus *Physisporinus vitreus* by means of
 308 response surface methodology. *Journal of Applied Microbiology* 106: 1734-1742.

309 Schubert, M., S. Mourad, S. Fink, and F. Schwarze, 2009. Ecophysiological responses of
 310 the biocontrol agent *Trichoderma atroviride* (T-15603.1) to combined
 311 environmental parameters. *Biological Control* 49: 84-90.

312 Schwarze, F., and H. Landmesser, 2000. Preferential degradation of pit membranes
 313 within tracheids by the basidiomycete *Physisporinus vitreus*. *Holzforschung* 54:
 314 461-462.

315 Schwarze, F., H. Landmesser, B. Zraggen, and M. Heeb, 2006. Permeability changes in
 316 heartwood of *Picea abies* and *Abies alba* induced by incubation with
 317 *Physisporinus vitreus*. *Holzforschung* 60: 450-454.

318 Sienkiewicz, N., T. Buultjens, N. White, and J. Palfreyman, 1997. *Serpula lacrymans* and
 319 the heat-shock response. *International Biodeterioration & Biodegradation* 39:
 320 217-224.

321 Skinner, G., J. Larkin, and J. Rhodehamel, 1994. MATHEMATICAL MODELING OF
 322 MICROBIAL GROWTH: A REVIEW. *Journal of Food Safety* 14: 175-217.

323 Trinci, A.P.J., 1974. A Study of the Kinetics of Hyphal Extension and Branch Initiation of
 324 Fungal Mycelia. *J Gen Microbiol* 81: 225-236.

325
 326 **Figure captions**

327 Figure 1: Fungal growth model. (a) The fungal growth model (FGM) considers hyphae and
 328 nutrients as discrete objects. Hyphae are root-like branching structures of the filamentous
 329 fungus and represented in the model by edges and nodes. (b) Starting from initial nodes the
 330 growth of the fungal colony is determined by key processes such as polarization, branching,
 331 uptake and concentration of nutrients and transport. Details about the model construction can
 332 be found in (Fuhr et al., 2010).

333 Figure 2: Model calibration. In order to calibrate the FGM we compare the simulation to
 334 laboratory experiments of *P. vitreus* cultivated on MEA and observed over 150 minutes by
 335 using WFM. The qualitative comparison of the growth front (a) *in vitro* and (b) *in silico* by

336 using the FGM with the parameter set given in Tab. 1 shows a good agreement. Quantitative
337 comparisons of total hyphal length of the mycelium, the number of active tips and the HGU
338 within the box are given in Tab. 2.

339 Figure 3: Effect of environment. Response of the fungus to different sets of water activity
340 levels and temperatures at pH 5. The filled symbols are the laboratory experiments
341 of (Schubert et al., 2010), i.e. the water activity levels are 0.998 (circle), 0.990 (triangle),
342 0.982 (square), 0.974 (diamond) and 0.970 (star). The solid lines with the empty symbols are
343 the corresponding simulation of the FGM by using $a = [0.0, 0.2, 1.0, 1.8, 6.4]$ and values of b
344 in the interval $[0.2, 4.0]$. Each solid line represents the average over 10 realizations and the
345 uncertainty of the data points is within the range of the symbols.

346 Figure 4: Growth pattern. (a) Morphologies of *P. vitreus* at water activity levels of 0.982,
347 0.990 and 0.999 from the left to the right at $T = 20^\circ\text{C}$ and $\text{pH} = 6$. (b) The corresponding
348 simulations show the fungal colony after approximately 24 hours of growth using $a = (0, 1,$
349 $1.8)$ and $b = 2$.

350 Figure 5: Parameter estimation. The model parameter a increases exponentially with
351 decreasing water activity levels.

352

353 **Table caption**

354 Table 1: Typical model parameters used throughout this work. We use the same notation as in
355 (Fuhr et al., 2010).

356 Table 2: Quantitative comparison of the experiment and the FGM shown in Fig. 2. The
357 evolution of the mycelium is measured *in vivo* over a time span of 150 minutes at a
358 temperature of approximately 20°C , $\text{pH} = 6$ and a water activity of 0.990. This experimental
359 condition corresponds to the FGM by using the parameters in Tab. 1.

360

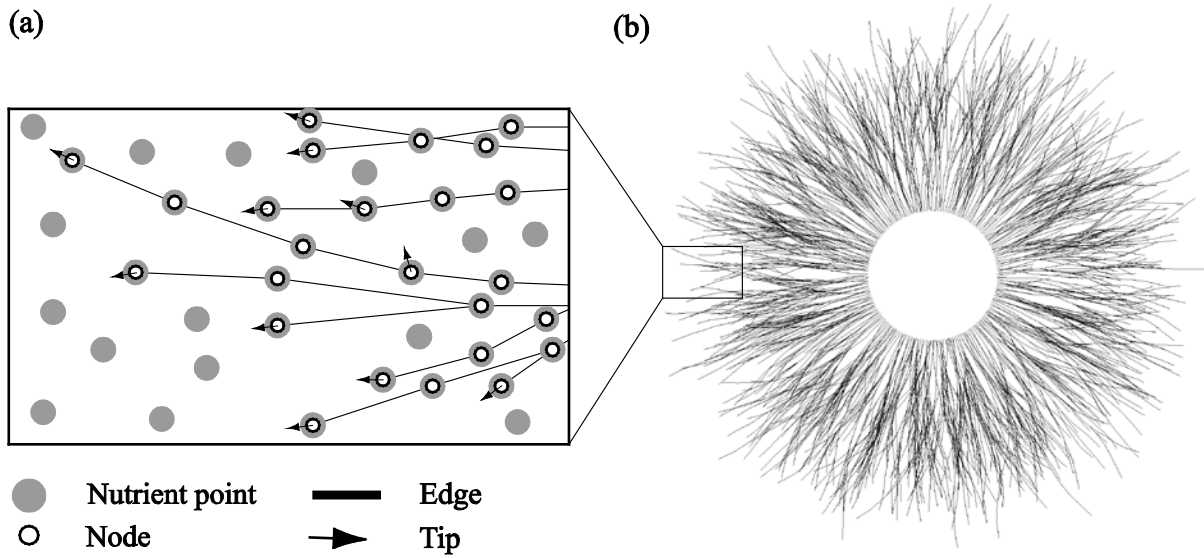


Fig.1: Abbildungen/Model/Model.eps
80 x 160 mm

Dieser Text ist in Times New Roman 12

Dieser Text ist in Times New Roman 12 B

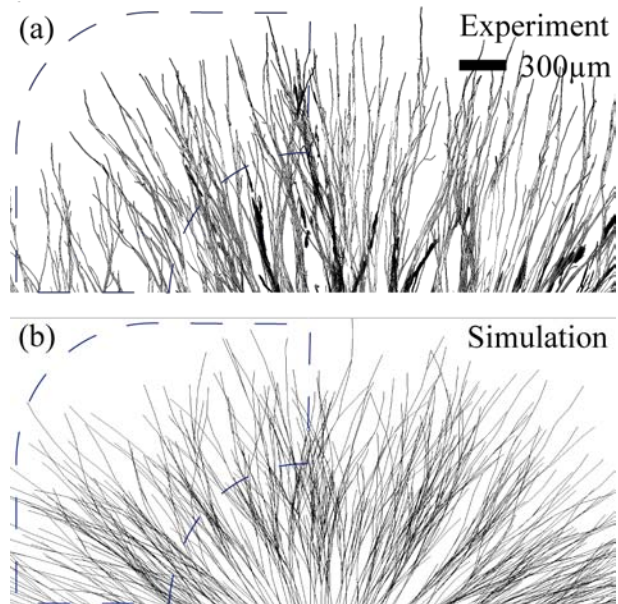


Fig. 2: Abbildungen/GrowthFront/GrowthFront_Box.png
80 x 80 mm

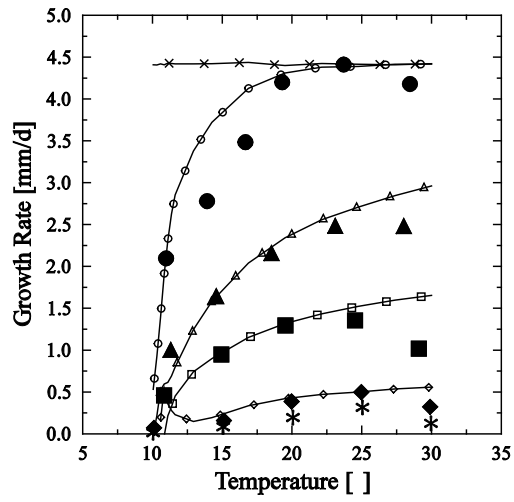


Fig. 3: /home/mfuhr/15_fungi3D/02_Models/20_2Dmorph/auswertung_22/PLOT_PAPER/temp_aw_20_2Dmoph.eps

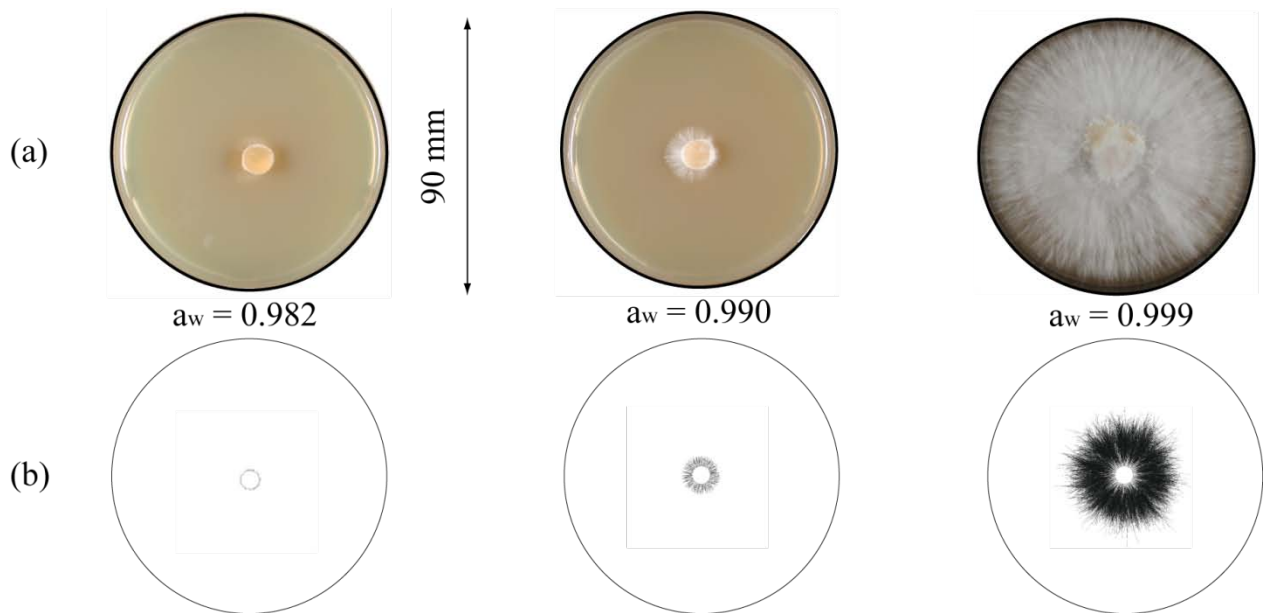


Fig. 4: Abbildungen/WaterActivity/WaterActivity1.png

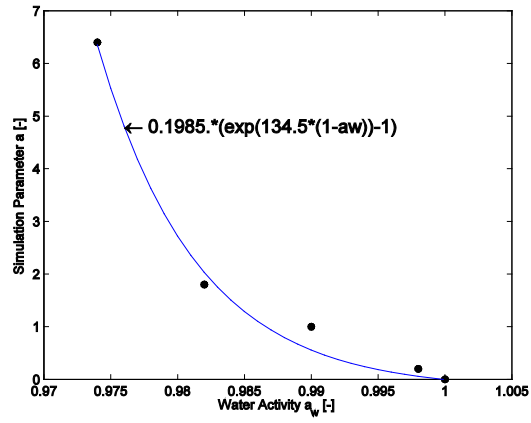


Fig. 5: /home/mfuhr/15_fungi3D/02_Models/20_2Dmorph/auswertung_22/FIT_a_b/
FIT_a.eps

Substrate:			
Box size $L \times L$	L	90	mm
Number of nutrient point	N_p	$1.6 * 10^7$	-
Poissonian distribution (interval = $2 * \xi$)	ω	2733	-
Fungus:			
Mean hyphal growth rate	μ	2.6	mm/d
Mean edge length	λ	$2/3 * \xi$	mm
Growth cut-off length	ξ	10	mm
Growth cut-off angle	θ	0.44	°
Growth costs (Eq. 2)	$[a,b]$	[1, 1.5]	-
Pit initial nutrient	v	$4 * 10^{-13}$	mol
Pit initial degradation rate	α_I	$v/20$	mol
Pit degradation rate	α_C	$0.45 * v$	mol/d
Apical branching threshold	β_t	$0.6 * v$	mol
Lateral branching threshold	β_s	$0.35 * v$	mol
Simulation:			
Initial number of pellet	n_k^0	200	-
Initial number of tips	n_s^0	1	-
Initial nutrient concentration	n_n^0	$3/2 * \beta_t$	mol

Table 1

	Symbol [unit]	Experiment	Model
Total hyphal length of mycelium	L_m [mm]	90	96
Number of active tips	N_t [-]	210 (\pm 50)	230
Hyphal growth unit	$HGU = L_m / N_t$ [μ m]	428 (\pm 90)	417
Radial growth rate	G_R [mm/d]	2	2.05

Table 2